Available online at www.sciencedirect.com
ScienceDirect
Journal of the European Ceramic Society 29 (2009) 2705–2711
www.elsevier.com/locate/jeurceramsoc

Transparent mullite ceramic from single-phase gel by Spark Plasma Sintering

Guimin Zhang [a,b], Yucheng Wang [a], Zhengyi Fu [a,*], Hao Wang [a], Weiming Wang [a], Jinyong Zhang [a], Soo Wohn Lee [c], Kochi Niihara [d]

[a] *State Key Lab of Advanced Technology for Materials Synthesis and Processing, Wuhan University of Technology, Wuhan 430070, PR China*
[b] *Department of Chemistry, School of Sciences, Wuhan University of Technology, Wuhan 430070, PR China*
[c] *Department of Materials Engineering, SunMoon University, Asar, ChungNan 336-708, Republic of Korea*
[d] *Extreme Energy Density Research Institute, Nagoka University of Technology, 1603-1, Kamitomioka, Nagoba, Niigata 940-2188, Japan*

Received 15 November 2008; received in revised form 2 April 2009; accepted 8 April 2009
Available online 14 May 2009

Abstract

Monophasic mullite precursors with composition of $3Al_2O_3{\cdot}2SiO_2$ (3:2) were synthesized and then were sintered by Spark Plasma Sintering (SPS) to form transparent mullite ceramics. The precursor powders were calcined at 1100 °C for 2 h. The sintering was carried out by heating the sample to 1450 °C, holding for 10 min. The sintered body obtained a relative bulk density of above 97.5% and an infrared transmittance of 75–82% in wavelength of 2.5–4.3 μm without any additive. When the precursor powders were calcined at below 1100 °C, it was unfavorable for completely eliminating the residual OH, H_2O and organic compound. However, when calcined temperature was too high, it was unfavorable either for full densification due to the absence of viscous flow of amorphous phase. At the same calcined temperature, the transmittance of sintered body was decreased with the increase of the sintering temperature above 1450 °C owing to the elongated grain growth.

Keywords: Sol–gel processes; Microstructure; Optical properties; Mullite

1. Introduction

Mullite, because of its optical translucency and other beneficial properties like high-temperature strength, thermal-shock resistance, low dielectric constant, can be applied as an ideal optical window material at elevated temperature.[1–3] As a transparent material, mullite has to meet the following requirements: (1) high chemical purity; (2) low porosity; (3) phase purity; (4) absence of amorphous films at grain boundaries and triple junctions; (5) fine grain size, all of which depend on raw materials, processing of prepared powders and sintering. The sol–gel process is an effective method to synthesize mullite precursors. In general, mixing at the atomic level is useful for low-temperature (<l000 °C) synthesis of mullite, but not for low-temperature sintering because of the low inter-diffusion rate of aluminum and silicon ions in mullite.[4] In contrast, precursors mixed at the nanometer scale are better suited for low-temperature (1250–1500 °C) densification through viscous deformation.[5,6] Klug prepared IR-infrared transparent mullite ceramic by hot-pressing at 1630 °C from 72 wt% Al_2O_3 composition and hot isostatic pressing at 1650 °C from 76 wt% Al_2O_3 composition.[7] Ohashi et al. fabricated visible spectrum to infrared translucent mullite by pressureless sintering at 1750 °C.[8] The precursors prepared by the above researchers were all diphase xerogels. Schneider et al. also got transparent mullite at 1650 °C by hot isostatic pressing using commercial fused-mullite.[9] Only Fang et al. achieved transparent mullite ceramic at a low-temperature of about 1300 °C by microwave sintering using aerogels of supercritical drying.[10] None of these precursors is attributed to be single-phase xerogels.

Spark Plasma Sintering is a newly developed method for obtaining fully dense and fine-grained transparent ceramic[11] whose high heating rate obtained by directly heating the die and powders using pulse electric current will effectively hold up grain growth. However, to date, the reports on transparent mullite ceramic fabricated by Spark Plasma Sintering (SPS) are limited. Imai et al. successfully fabricated the translucent mullite–amorphous composite, which was not pure mullite

* Corresponding author at: State Key Lab of Advanced Technology for Materials Synthesis and Processing, Wuhan University of Technology, Wuhan 430070, PR China.
E-mail addresses: zyfu@whut.edu.cn (Z. Fu), zhangguimin2006@163.com (G. Zhang).

0955-2219/$ – see front matter © 2009 Elsevier Ltd. All rights reserved.
doi:10.1016/j.jeurceramsoc.2009.04.012

ceramic, from the metakaoline powder by SPS[12] by heating to 1300 °C at heating rate of 100 °C/min and pressure of 40 MPa. In the present study, transparent mullite ceramic has been fabricated in mid-infrared and visible light ranges from monophasic precursors by SPS. The effects of calcination temperature to precursor powders and sintering process on optical property and microstructure will also be discussed.

2. Experimental procedures

2.1. Preparation of samples

Monophasic gels with stoichiometric composition of the mullite (Al:Si = 3:1) were prepared from aluminum nitrate nanohydrate (ANN) and tetraethoxysilane (TEOS). The procedure for synthesizing gels is as follows: 56.271 g of ANN was dissolved in 50 ml of absolute ethanol and stirred at 60 °C for 24 h under reflux. The stoichiometric amount of TEOS dissolved in EtOH in advance was then added into the above solution and was stirred under reflux at 60 °C for 4 days. The amount of H_2O for hydrolysis and condensation of TEOS was provided by ANN. After refluxing, the resulting mixture was poured into a beaker, covered with filter paper and aged for around 5 days until the mixing solution became viscous. The finally obtained gel was dried at 110 °C for 2 days and then was crushed and ground to powders with alumina mortar and pestle. The powder was screened through a 54 μm sieve. The precursor powders were calcined at 800–1400 °C for 2 h at the rate of 10 °C/min.

The 2.5 g of calcination powders were poured into a graphite mold (inner diameter of 15 mm, outer diameter of 40 mm) and sintered at a temperature from 1450 °C to 1600 °C for 5–20 min by SPS (Model SPS-3.20MK II, Japan) at a heating rate of 100 °C/min in vacuum atmosphere. The temperatures of the samples during sintering were measured by an optical pyrometer focused on the sintered sample through a small hole in the mold. A pressure of 30 MPa was applied onto the samples from the beginning of the sintering process. The thickness of sintered specimens was about 3 mm.

2.2. Methods of characterization

Differential scanning calorimeter (DSC) analysis (STA-449C, Netzsch, German) was carried out in air at a heating rate of 10 °C/min. X-ray diffraction analysis (D/MAX-RB, Rigaku, Japan) was performed at 40 kV and 40 mA using a graphite monochromatic Cu K_α radiation at a range of 2θ from 10° to 90°, with a step size of 0.02° and a rate of 4°/min. Densities of the sintered samples were determined using the Archimedes method. Relative bulk densities were calculated by taking the theoretical density of mullite as 3.17 g/cm^3. The sintered bodies were sliced (0.6 mm in thickness) and polished for measuring infrared transmittance analysis with spectrometer (AVATAR370, Nicolet, USA). The samples were thermally etched for observing the microstructure using scanning electron microscopy (S-3400, Hitachi, Japan).

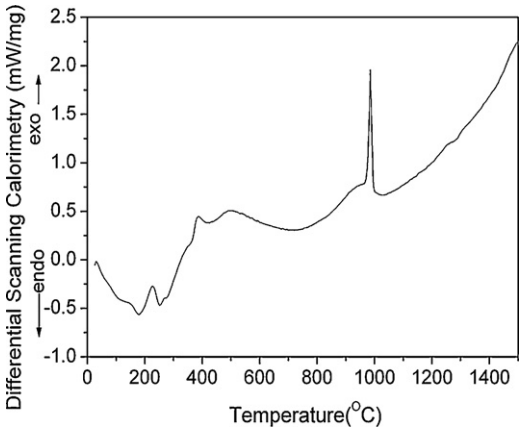

Fig. 1. DSC curve for mullite xerogel heated at 10 °C/min.

3. Results and discussion

3.1. Thermal evolution of precursor powders

Fig. 1 shows the DSC curve of mullite xerogel. A unique sharp exothermic peak at around 980 °C occurs. There is a very small exothermic peak that can be hardly perceptible at around 1200 °C, which is consistently recognized as the reaction sign between the formed spinel and amorphous silica. Fig. 2 shows XRD patterns of heated powders at different temperatures between 900 °C and 1400 °C for 2 h. Powders dried at 110 °C are in the amorphous state and retain the state until 950 °C. Above this temperature, precursors transform to mullite crystal and no spinel can be observed. The result is in good agreement with DSC analysis. It implies that mullite crystallization is formed directly from amorphous precursors without intermediate formation of Si, Al-spinel or γ-Al_2O_3. The gels can be assigned to type I mullite precursor.[13] However, there is a very low degree of reflection splitting of reflection pairs 1 2 0/2 1 0, 2 4 0/4 2 0, 0 4 1/4 0 1, and 2 5 0/5 2 0 at 1000 °C. Reflection splitting occurred with the increase of calcinations temperature and

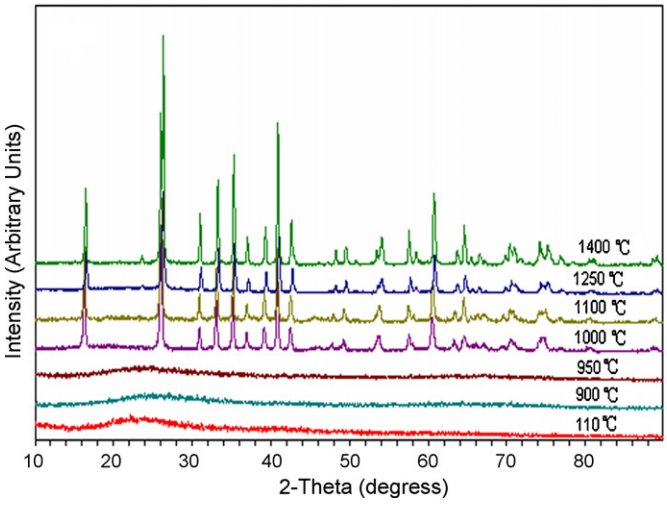

Fig. 2. XRD patterns of mullite precursor powders calcined at different temperatures for 4 h.

Table 1
d-Spacings of reflection pairs of samples calcined at different temperatures for 4 h.

Temperature (°C)	*d* (nm)							
	(1 2 0)	(2 1 0)	(2 4 0)	(4 2 0)	(0 4 1)	(4 0 1)	(2 5 0)	(5 2 0)
1000	0.34159	0.33985		0.16976	0.15989		0.14364	
1100	0.34140	0.33885		0.16974	0.15998		0.14388	
1250	0.34270	0.33959	0.17123	0.16981	0.15990	0.15811	0.14426	0.14264
1400	0.34194	0.33807	0.17122	0.16920	0.15993	0.15773	0.14246	0.14038

became more and more remarkable. Tables 1 and 2 show respectively *d*-spacings of reflection pairs at different temperatures and differences between *d*-spacings of reflection pairs at different temperatures. From Table 2 it can be seen that the differences are more obvious with the increase of temperature which means that the precursors form Al_2O_3-rich pseudotetragonal mullite at 1000 °C and the Al_2O_3-rich mullite gradually transforms to 3:2 orthorhombic mullite up to 1400 °C. It also indicates a part of the amorphous silica does not take part in the reaction at low-temperature and coexists with mullite which can be observed from the pattern of XRD at low-temperature as shown in Fig. 2. Jaymes et al. also verified the existence of amorphous silica in the mullite of low-temperature with ^{27}Al and ^{29}Si MAS-NMR spectroscopy.[14] Kleebe et al. analyzed the composition of grass pocket in mullite ceramic with electron energy-loss spectroscopy (EELS).[15] They found the grass pocket contain alumina and silica.

3.2. Densification behavior

Fig. 3 shows the effect of sintering temperature on relative density of sintered bodies. Among various holding times, the relative densities of samples sintered at 1500 °C are always highest and decrease with the increase of sintering temperature when temperature is above 1500 °C. Klug[6] thought this was due to the amount increasing of glass phase because the content of Al_2O_3 in mullite crystalline increases with the increase of temperature when the sintering temperature is above 1600 °C. However, in this study, the sintering temperature of all samples is lower than 1600 °C. Yu et al. thought the reason that the density decreased with the increase of temperature was due to the anisotropic grain growth.[16,17] This interpretation is verified with the microstructure of samples (as shown later). Fig. 3 also shows the effect of holding time on relative density. Among the three holding times (i.e. 5 min, 10 min and 20 min), the relative densities of

Table 2
Differences between *d*-spacings of reflection pairs of samples calcined at different temperatures for 4 h.

Temperature (°C)	Δ*d* (nm)			
	$d_{(120)} - d_{(210)}$	$d_{(240)} - d_{(420)}$	$d_{(041)} - d_{(401)}$	$d_{(250)} - d_{(520)}$
1000	0.0174			
1100	0.0255			
1250	0.0311	0.0142	0.0182	0.0162
1400	0.0387	0.0202	0.0220	0.0208

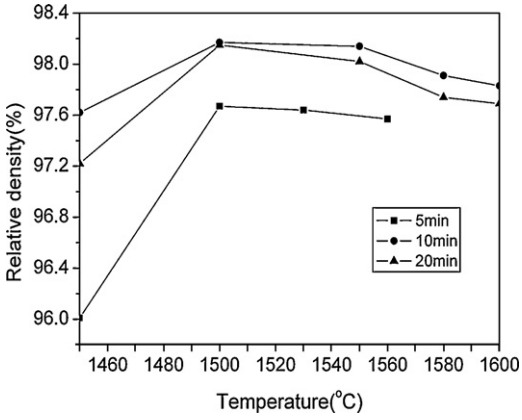

Fig. 3. Effect of sintering temperature and holding time on relative density of sintered bodies (precursor powders were calcined at 1000 °C).

samples sintered at any temperature for 10 min are the highest. This is because, the sintering process cannot be accomplished if the holding time is equal or less than 5 min, whereas, holding time longer than 10 min will facilitate the rapid growth of the elongated grains and intragranular holes. Thus, the appropriate holding time is 10 min according to this study.

The effect of calcination temperature on the relative density is shown in Fig. 4. From Fig. 4 it is found that the densities of the samples decrease with the increase of calcination temperatures. The highest density is achieved when powders are calcined at 800 °C, at which, mullite had not been formed. In order to clearly interpret the effect of calcination temperature on the relative densities, Fig. 5 shows the relation of the displacement which reflects the size deformation of the sample in sintering process

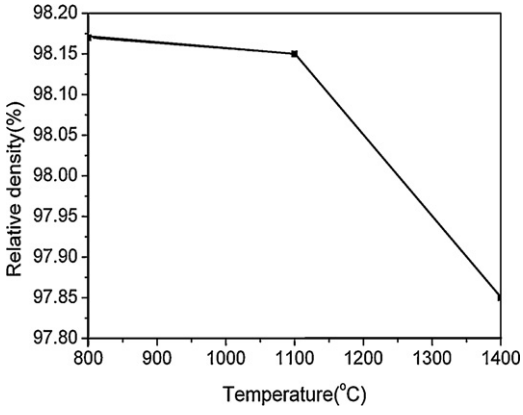

Fig. 4. Effect of calcination temperature on relative densities of sintered bodies (samples are sintered at 1450 °C for 10 min by SPS).

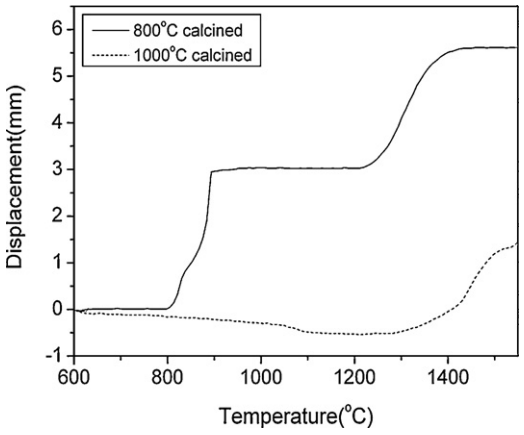

Fig. 5. Relationships between displacement and sintering temperature for samples calcined at different temperatures (the samples were sintered at 1550 °C for 10 min).

and sintering temperature of two different samples formed at different calcination temperatures. It should be noted that the displacements of those samples are almost the same when the precursor powders are calcined above 1000 °C, at the temperature the precursors has transformed into mullite crystal. So only the displacement-sintering temperature curve of powder compact calcined at 1000 °C is adopted to compare with that of the compact calcined at 800 °C. The positive and negative values of the vertical coordinate mean the shrinkage and dilation of the samples, respectively. The sample calcined at 800 °C shows two stages of densification (i.e. shrinkage). In the first stage, there is an abrupt shrinkage at around 900 °C which is corresponding to the formation of mullite. This is a phase transformation sintering process. There is no further densification behavior as soon as the mullite has formed and the samples shrink very little from 950 °C to 1250 °C. Above 1250 °C, the second stage of densification takes place. The samples finish densification at around 1425 °C and do not shrink any more. The samples calcined at 1000 °C do not undergo the first stage of densification because the powders have been transformed into mullite in the process of calcination so that no phase transformation occur at about 900 °C in the sintering process. For the second stage, samples calcined above 1000 °C undergo the densification process at the similar temperature as the samples calcined at 800 °C. These phenomena have reasonably interpreted why under the same sintered temperature, the relative density of the sintered body from 800 °C calcination temperature is higher than that from above 1000 °C (also see Fig. 4). For powders calcined at 1000 °C, although mullite forms, amorphous silica still exists (discussed in Section 3.1). In the condition of high heating rate in SPS, amorphous silica has no enough time to diffuse into mullite or react with alumina to form into mullite. When sintering temperature is above 1250 °C, the viscosity of amorphous phase decreases sharply with the increase of sintering temperature.[18,19] So the main sintering mechanism was still the viscous flow of the amorphous phase. Only in the stage of holding at final temperature, when all of amorphous phase almost transform into mullite, solid-state diffusion play a main role in the densification process. This is the reason why relative densities of samples sintered at 1450 °C are over 97.5% by SPS, while it is difficult to be sintered to full densification for monophasic mullite gel by other sintering methods such as hot-pressing, pressureless sintering, and so on. For the samples calcined at higher temperature, the amount of the amorphous phase decreases with the increase of calcination temperature. Viscous flow of the sintering mechanism plays less and less role. On the other hand, the rate of solid-state diffusion is slow when the sintering temperature is below 1450 °C. So the relative densities of samples calcined up to 1000 °C decrease with calcination temperature. When the precursor powders are calcined at 1400 °C, the chemical composition of the formed mullite is near 3:2, the amount of amorphous phase is very limited. The absence of amorphous phase is unfavorable to densification.

3.3. Microstructure

Fig. 6 shows microstructures of mullite ceramics sintered at different temperatures for 10 min. All precursor powders of samples were calcined at 1000 °C. Sintered at 1450 °C, the sample has a microstructure of fine, nearly equiaxial grains with an homogenous size of 0.1–0.5 μm (Fig. 6(a)). Sintered at 1500 °C, abnormal grain growth occurs, leading to a microstructure consisting of small proportion of elongated grains and some rectangular grains in a matrix of fine equiaxial grains. However, the grains grow slowly with the highest length of 5 μm and width of 2 μm (Fig. 6(b)). When sintering temperature is increased to 1550 °C, both elongated and equiaxial grow distinctly. The average size of equiaxial grain is 1.5 μm and the greatest length size of elongated grain is 20 μm (Fig. 6(c)). Further heating to 1600 °C, proportion of elongated grains increase apparently and grains become bigger. Some intragranular pores are engulfed in elongated mullite grains due to grains rapid growth (Fig. 6(d)). This is the reason why the relative densities of sintered bodies decrease with the increase of sintered temperature.

3.4. Appearance of sintered mullite ceramic slices and IR transmittance

Fig. 7 shows the appearance of mullite ceramic sintered at various temperatures from precursors calcined at different temperatures. If the precursors are calcined at 800 °C and the sample is sintered at 1450 °C for 10 min, the final product is white and completely opaque. If the calcination temperature is 1000 °C, sample sintered under the same condition, the final product is transparent. It can be seen from Fig. 7 the characters under the slices are clearly legible. However, the heterogeneity in color is more and more distinct with the increase of sintering temperature. Sintered at 1550 °C (under calcination temperature of 1000 °C), the sample becomes black and opaque. All specimens except that calcined at 800 °C have a gray or black rim in the outer layer, approximately 0.5 mm in width. This is due to the penetration of carbon to the sample from the mold by diffusion. Increasing sintering temperature promotes diffusion of carbon so that specimens dissolve a considerable quantity of carbon. It drops transmittance of specimens in visible light scope.

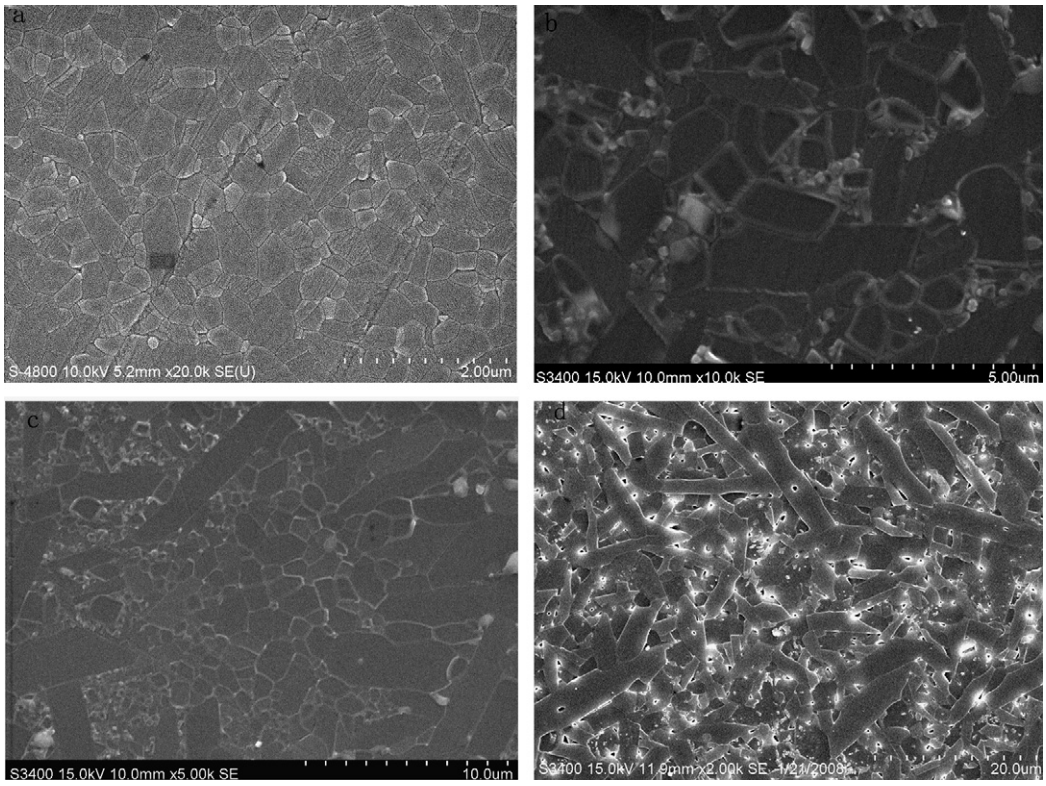

Fig. 6. SEM observations of microstructure of mullite ceramics sintered at (a) 1450 °C, (b) 1500 °C, (c) 1550 °C, (d) 1600 °C ((a–c) thermally etched at 1350 °C and (d) thermally etched at 1400 °C). (All samples are from precursor powders calcined at 1000 °C. They are hold at highest temperature for 10 min.)

Fig. 8 shows the effect of sintered temperature on transmittance of specimens for the holding times of 10 min and 20 min, respectively. Basically, the results shown in Fig. 8 are accorded with the above appearance. The transmittance decreases with the increase of sintering temperature for different holding times. The longer holding time result in the decrease of transmittance more obviously. From the above analyses, we can clearly see that the effect of microstructures on transmittance is more significant than that of the relative density in mullite ceramic system. The elongated grains dramatically decrease the transmittance of samples.

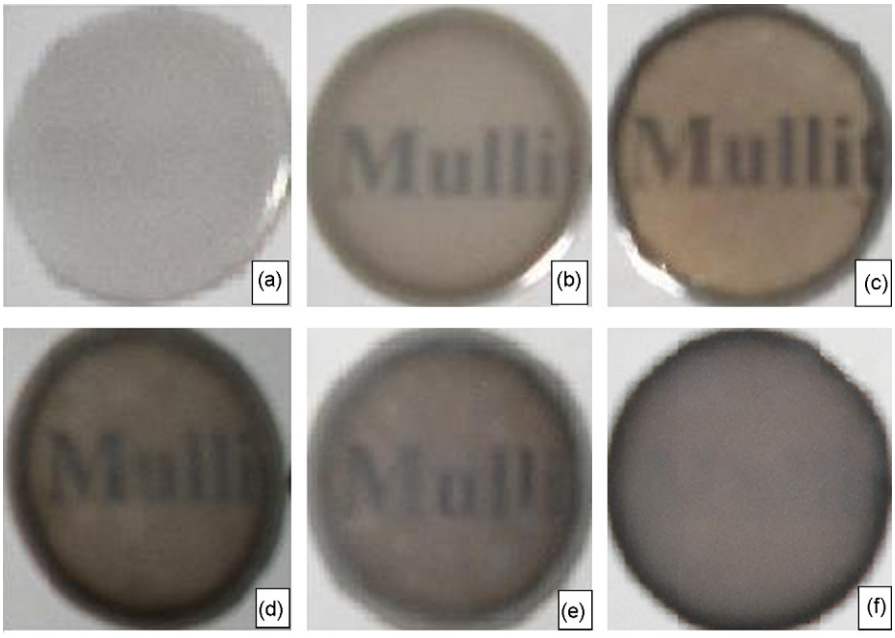

Fig. 7. Appearance of sintered mullite ceramic ((a–d) sintered at 1450 °C for 10 min. (a) 800 °C calcined, (b) 1000 °C calcined, (c) 1100 °C calcined, (d) 1400 °C calcined, (e) sintered at 1500 °C, (f) sintered at 1550 °C and (e and f) calcined at 1000 °C).

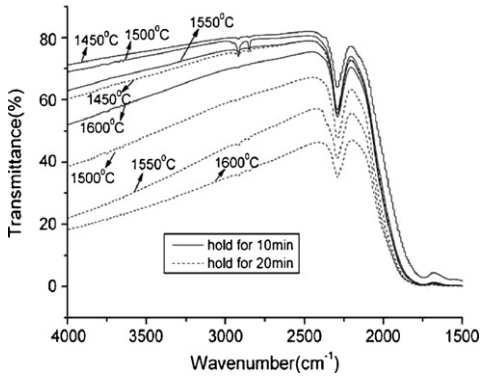

Fig. 8. Effect of sintering temperature and holding time on transmittance of mullite ceramic (precursor powders were calcined at 1000 °C).

Fig. 9 shows the effect of calcination temperature on transmittance. Transmittances of specimens calcined at 1000 °C, 1100 °C and 1200 °C are nearly identical, the results for the specimen calcined at 1100 °C are shown in Fig. 8. The highest transmittance of the specimen is from powders calcined at 1100 °C. This specimen has the transmittance of 75–82% in wavelength of 2.5–4.3 μm. The transmittance of the specimen calcined at 800 °C is the lowest, although its relative density is the highest. From the transmittance spectra, the sample calcined at 800 °C has another three absorption peaks at around 3580 cm^{-1}, 3450 cm^{-1} and 2700 cm^{-1}. Bands centered at around 3580 cm^{-1} and 3450 cm^{-1} are attributed to the stretching vibrations of –OH and H_2O. Schneider also found that –OH and H_2O existed in precursors calcined at 900 °C.[20,21] Bands at 2700 cm^{-1} should be attributed to the stretching mode of C=O which comes from oxidation product of residual organic compound. The results indicate that the residual –OH, H_2O and organic compound dramatically decrease transmittance of specimen. These absorption peaks at 3580 cm^{-1}, 3450 cm^{-1} and 2700 cm^{-1} are small or absent in specimens calcined at temperature above 1000 °C, which suggests that –OH, H_2O and organic compound in the precursors calcined above 1000 °C have been eliminated in the calcining process. The transmittance of specimen calcined at 1400 °C also decreases distinctly. This is because higher calcinations temperature will result in a lower surface area of powders and hard agglomerates, both of which are unfavorable for packing.[5,22] On the other hand, it should be noted that the chemical composition of mullite of near 3:2 causes absence of amorphous silica, which contributes to the viscosity flow mechanism in lower calcinations temperature.

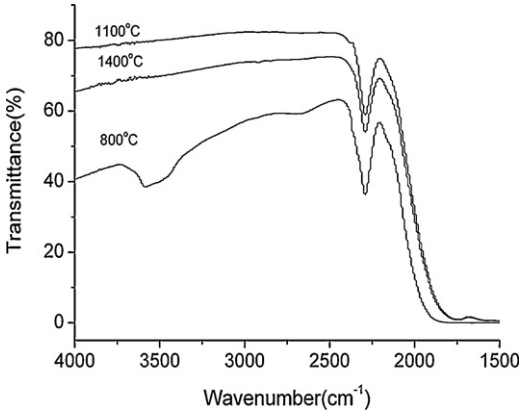

Fig. 9. Effect of calcination temperature on transmittance of mullite ceramic (samples are sintered at 1450 °C for 10 min by SPS).

4. Conclusions

In this study, it had been shown that the single-phase mullite gels can be prepared by the slow hydrolyses of tetraethoxysilane and aluminum nitrate nonahydrate. The precursors crystallized to Al_2O_3-rich pseudotetragonal mullite directly from amorphous state at about 980 °C. They gradually transform to 3:2 orthorhombic mullite with the increase of temperature. Infrared-transparent mullite ceramics is fabricated from the monophasic gels by SPS. Based on the precursors calcined at 1100 °C, the transmittance of specimen sintered at 1450 °C for 10 min is 75–82% in 2.5–4.3 μm wavelength range. It was found that, lower calcined temperature of the precursors are unfavorable for eliminating residual –OH, H_2O and organic compound, which may dramatically decrease the transmittance of specimen. Whereas, when the precursors are calcined at higher temperature, absence of the amorphous silica has detrimental effect on full densification. Specimen sintered at 1450 °C provides fine equiaxial grains with homogenous size of submicrometer which results in high transmittance. Too high sintering temperature will lead to a great deal of elongated grains distributed in the matrix of granular grains. Elongated grains and penetration of carbon yielded at higher sintering temperature decrease transmittance in visible light and infrared range.

Acknowledgements

The authors thank the National Nature Science Foundation of China (50772081, 50821140308) and the Ministry of Education of China (PCSIRT0644) for financial support of the research.

References

1. Schneider, H., Schreuer, J. and Hildmann, B., Structure and properties of mullite—a review. *J. Eur. Ceram. Soc.*, 2008, **28**, 329–344.
2. Aksay, IIhan, A., Dabbs, Daniel, M. and Sarikaya, M., Mullite for structural, electronic, and optical applications. *J. Am. Ceram. Soc.*, 1991, **74**, 2343–2358.
3. Schneider, H. and Komarneni, S., *Mullite*. Wiley–VCH, Weinheim, 2005, pp. 1–487.
4. Amutharani, D. and Gnanam, F. D., Low temperature pressureless sintering of sol–gel derived mullite. *Mater. Sci. Eng.*, 1999, **A264**, 254–261.
5. Ivankovica, H., Tkalcec, E., Nass, R. and Schmidt, H., Correlation of the precursor type with densification behavior and microstructure of sintered mullite ceramics. *J. Eur. Ceram. Soc.*, 2003, **23**, 283–292.
6. Ebadzadeh, T., Formation of mullite from precursor powders: sintering microstructure and mechanical properties. *Mater. Sci. Eng.*, 2003, **A355**, 56–61.
7. Prochazka, S. and Klug, F. J., Infrared transparent mullite ceramic. *J. Am. Ceram. Soc.*, 1983, **66**, 874–880.
8. Ohashi, M., Tabata, H., Abe, O. and Kanzaki, S., Preparation of translucent mullite ceramics. *J. Mater. Sci. Lett.*, 1987, **6**, 528–530.
9. Schneider, H., Schmuecker, M., Ikeda, K. and Kaysser, W. A., Optically translucent mullite ceramic. *J. Am. Ceram. Soc.*, 1995, **76**, 2912–2914.

10. Fang, Y., Roy, R., Agrawal, D. K. and Roy, D. M., Transparent mullite ceramics from diphasic aerogels by microwave and conventional processings. *Mater. Lett.*, 1996, **28**, 11–15.
11. Xiong, Y., Fu, Z. Y., Wang, H., Wang, W. M., Zhang, J. Y., Zhang, Q. J. *et al.*, Translucent Mg-a-Sialon ceramics prepared by spark plasma sintering. *J. Am. Ceram. Soc.*, 2007, **90**, 1647–1649.
12. Imai, T., Naitoh, Y., Yamamoto, T. and Ohyanagi, M., Translucent nano mullite based composite fabricated by spark plasma sintering. *J. Ceram. Soc. Jpn.*, 2006, **114**, 138–140.
13. Schneider, H., Voll, D., Saruhan, B., Sanz, J., Schrader, G. and Ruscher, C., Synthesis and structural characterization of non-crystalline mullite precursors. *J. Non-Cryst. Solids*, 1994, **178**, 262–271.
14. Jaymes, I., Douy, A., Massiot, D. and Coutures, J. P., Characterization of mono- and diphasic mullite precursor powders prepared by aqueous routes 27Al and 29Si MAS-NMR spectroscopy. *J. Mater. Sci.*, 1996, **31**, 4581–4589.
15. Kleebe, H. J., Hilz, G. and Ziegler, G., Transmission electron microscopy and electron energy-loss spectroscopy characterization of glass phase in sol–gel-derived mullite. *J. Am. Ceram. Soc.*, 1996, **79**, 2592–2600.
16. Yu, J., Shi, J. L., Yuan, O. M., Yang, Z. F. and Chen, Y. R., Effect of composition on the sintering and microstructure of diphasic mullite gels. *Ceram. Int.*, 2000, **26**, 255–263.
17. Hong, S. H. and Messing, G. L., Anisotropic grain growth in diphasic-gel-derived titania-doped mullite. *J. Am. Ceram. Soc.*, 1998, **81**, 1269–1277.
18. Kara, F. and Little, J. A., Sintering behaviour of precursor mullite powders and resultant microstructures. *J. Eur. Ceram. Soc.*, 1996, **16**, 627–635.
19. Kara, F. and Sener, O., Improvement of sintering and microstructural homogeneity of a diphasic mullite. *J. Eur. Ceram. Soc.*, 2001, **21**, 901–905.
20. Voll, D., Beran, A. and Schneider, H., Temperature-dependent dehydration of sol–gel-derived mullite precursors: an FTIR spectroscopic study. *J. Eur. Ceram. Soc.*, 1998, **18**, 1101–1106.
21. Berana, A., Voll, D. and Schneider, H., Dehydration and structural development of mullite precursors: an FTIR spectroscopic study. *J. Eur. Ceram. Soc.*, 2001, **21**, 2479–2485.
22. Kamiya, H., Suzuki, H., Ichikawa, T., Cho, Y. C. and Horio, M., Densification of sol–gel-derived mullite ceramics after cold isostatic pressing up to 1 GPa. *J. Am. Ceram. Soc.*, 1998, **81**, 173–179.